Characterizing the Effects of *stm* and *ath1* Mutations on Floral Organ Development in *Arabidopsis thaliana*

By:
James Leary

A thesis submitted to the faculty of The University of Mississippi in partial fulfillment of the requirements of the Sally McDonnell Barksdale Honors College.

Oxford
May 2,2018

Approved by:

_____
Advisor: Dr. Sarah Liljegren

_____
Reader: Dr. Jason Hoeksema

_____
Reader: Dr. Colin Jackson

ACKNOWLEDGEMENTS

I would like to first thank Dr. Liljegren for accepting me into her lab a year and a half ago and for mentoring me throughout this whole process. I have no doubt that the experience I have gained working in this lab has not only helped me achieve my goals thus far but also will continue to benefit me in the pursuit of my professional goals.

I would also like to thank all of the other members of the Liljegren lab team. It is in large part in thanks to your constant support and aid that I was able to complete this project. I want to show my gratitude to Emily Fountain, Greta Parker, and Adam Harris for helping me to learn the protocols as well as being there to aid me whenever needed. To Hunter Roth, Hayden Malone, Kate Childers, Sam Palmer, and Jack Mason, the other students who worked in the lab, thank you for making this whole experience so enjoyable.

Though all of my research took place inside of the lab I could not have completed this project without the support of my family and friends. Thank you for holding me accountable while also constantly supporting me, I can sincerely say that I appreciate everything that you all have done for me.

Lastly, I would like to show my gratitude to the Sally McDonnell Barksdale Honors College. Thank you for all of the opportunities granted to me over the course of my undergraduate education, in particular the opportunity to complete this thesis. I know that the experience will influence the rest of my scholastic career and I am appreciative to have completed it.

This research was supported by an NSF grant (IOS-1453733) to SL.

ABSTRACT

JAMES LUKE LEARY: Characterizing the Effects of *stm* and *ath1* Mutations on Floral Organ Development in *Arabidopsis thaliana*(Under the direction of Dr. Sarah Liljegren)

The purpose of this project was to explore the function of SHOOTMERISTEMLESS (STM) and ARABIDOPSIS THALIANA HOMEOBOX GENE1 (ATH1), two transcription factors in *Arabidopsis thaliana* that play a role in the molecular pathways that establish organ boundaries in flowers. Prior research has shownthat mutations in the *STM* and *ATH1* genes cause defects in the boundaries formed between floral organs and the stem of the plant. My study was designed to investigate whether ATH1 and STM also control the boundaries found between adjacent floral organs. I predicted that *stm ath1-3* double mutant flowers would display a significant number of stamen-stamen and sepal-sepal fusion events compared to wild-type flowers, which would indicate that the boundaries between these organs had been compromised.

Stem cells found in flower meristems are required for a full set of floral organs to develop. Since STM are ATH1 are known to play roles in maintaining the population of stem cells in both shoot and flower meristems, *stm ath1-3* double mutant flowers were also expected to produce fewer organs compared to wild-type flowers. I found that 15 percent of the stamens in *stm* and *ath1-3* single mutant flowers, and 51 percent of the stamens in *stm ath1-3* double mutant flowers were fused to another stamen. I also found that 95 percent of the sepals in the double mutant flowers were fused to a neighboring sepal. The *stm ath1-3* mutant flowers produced three fewer petals and three fewer stamens on average. These results indicate that STM and ATH1 redundantly regulate boundaries formed between stamens and petals. They also demonstrate that STM and

ATH1 regulate the size of the flower meristem and that their functions are required for that meristem to correctly produce all of its organs.

TABLE OF CONTENTS

LIST OF FIGURES AND TABLES

LIST OF ABBREVIATIONS

A. thaliana: *Arabidopsis thaliana*

SAM: shoot apical meristem

DNA: deoxyribonucleic acid

WT: Wildtype

ATH1: *ARABIDOPSIS THALIANA* HOMEBOX GENE 1

***ath1*:** *ATH1* mutant

STM: SHOOT MERISTEMLESS

stm: *STM* mutant

Ler: Landsberg *erecta*

mRNA: messenger RNA

PCR: polymerase chain reaction

T-DNA: transfer DNA

PNY: PENNYWISE

PNF: POUND-FOOLISH

***pny*:** *PNY* mutant

pnf: *PNF* mutant

INTRODUCTION

When considering the complex and consistent nature in which a plant grows flowers, one must consider the genomic pathways that are responsible for this phenomenon. Each flower is subject to specific genetic regulations that are influential in the development of floral organs (Meinkeet al., 1998**)**. Through study of these genomic pathways and genetic regulations, understanding can be found regarding the development of flowers.

Arabidopsis thaliana is a plant species that is known for the various genomic properties that it has; in particular, these properties lend it to being one of the better-known model organisms for genetic research. Some of these reasons are its relatively small genome, rapid life cycle, prolific seed production, efficient transformation methods, large number of mutant lines and genetic resources, and economic, accessible requirements for growth**.** Many genes are conserved between multiple plant species; therefore, understanding the roles that specific genes play in *Arabidopsis thaliana* can give us extensive insight into plant biology as a whole (Meinkeet al., 1998**)**.

The number of floral organs in *Arabidopsis thaliana* is conserved between plants, as is the relative position of the floral organs (**Figure 1**). Typically a flower of a wildtype plant is composed of four sepals, four petals, six stamens, and two fused carpels. Each of these categories are found in a whorl, which is an arrangement of organs that radiate from a single point and encircle the stem (Irish et al., 1999). In wildtype plants, there are distinctive lateral boundaries found that separate each of these organs from the floral stem (Gomez-Mena and Sablowski, 2008). These organs and their growth pattern can be seen in **Figure 1.**

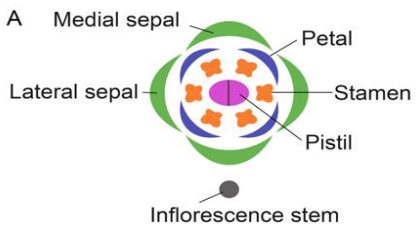

Figure 1: Diagram of the floral organs present in an *Arabidopsis thaliana* flower. A 'top-down' look at an *A. thaliana* flower that shows the location of petals, sepals, and stamens. A wildtype flower typically has four petals, four sepals, and six stamens that surround a central pistil. (Image credit: Gubert et al., 2014)

Multipotent stem cells found within the tip of a developing shoot make up the shoot apical meristem (SAM). Flower primordia formed on the flanks of a shoot meristem also contain sufficient stem cells to form the distinct organ types of a flower (Barton, 2010). The boundaries of these organs are made up of layers of densely packed cells that serve to separate distinct tissues. The cells of these dense layers are generally smaller in size than the cells surrounding the regions (Breuil-Broyer et al., 2004). Multiple types of organ boundaries are found in a flower. Lateral organ boundaries are groups of cells at the adaxial base of the floral organs (ie. sepal-stem), while inter-organ boundaries separate adjacent organs within the same whorl (ie. sepal-sepal) and inter-whorl boundaries distinguish organs in neighboring whorls (ie. petal-stamen)(Shuai et al., 2002).Genetic screens in *Arabidopsis* have uncovered mutants that alter each of these boundaries. (Arnaud and Pautot, 2014)

A transcription factor recognized to play a role in the formation of lateral and inter-organ boundary regions in *Arabidopsis* flowers is encoded by the *ARABIDOPSIS THALIANAHOMEOBOX GENE1* (*ATH1*) gene (Gomez-Mena and Sablowski, 2008; Liljegren,

unpublished results). ATH1is a BELL-type homeodomain transcription factor that represses growth of the basal regions of floral organs that border the floral receptacle (upper part of the floral stem). Mutations in *ATH1* hamper the process of lateral organ boundary formation, and the boundary region between the sepals and floral stem is less distinct. The stamens of *ath1* single mutant flowers are frequently fused at their bases to the underlying receptacle, and fail to detach during the abscission process (Gomez-Mena and Sablowski, 2008; Liljegren, unpublished results). Adjacent stamens of *ath1* flowers are sometimes fused along part of their filaments, which is an inter-organ boundary defect. The mutant alleles referred to in this study, *ath1-3* and *ath1-5*, both introduce errors in the DNA-binding region of the protein (**Figure 2**).

SHOOTMERISTEMLESS (STM) is a KNOX-type homeodomain transcription factor essential for formation of the shoot meristem and its sustained activity, such as stem cell proliferation (Long et al., 1996). STM does this by activating cytokinin biosynthesis in the shoot meristem (Scofield et al., 2014). Within the developing flower, STM causes a delay in the differentiation of organ primordia and, like ATH1, represses growth to allow floral organ boundaries to be established (Aida et al., 1999). Previous studies have shown that loss-of-function mutations of *STM* lead to an absence of the SAM as well as fusions between the cotyledons of *stm* seedlings (Scofield et al., 2014).

Since the loss-of-function alleles have such a severe effect on plant development, partial loss of function alleles have been studied to further examine the roles of STM. For instance, the flowers produced by a weak *stm-2* allele contain fewer total floral organs (Endrizzi et al., 1996).These results show that when *stm* mutants retain enough shoot meristem function to produce flower meristems on their flanks, the flowers reveal defects indicative of flower meristem maintenance issues. The hypomorphic *stm* mutant used in this study is caused by a

point mutation that introduces a premature stop codon in the homeodomain region of the STM transcription factor, seen in **Figure 2** (Liljegren, unpublished results). The phenotype of this *stm* mutant mimics that of the *ath1* mutants described above, with reduced definition of the lateral organ boundaries between the sepal and floral stem, and fusion of the stamens to the underlying stem, preventing their detachment.

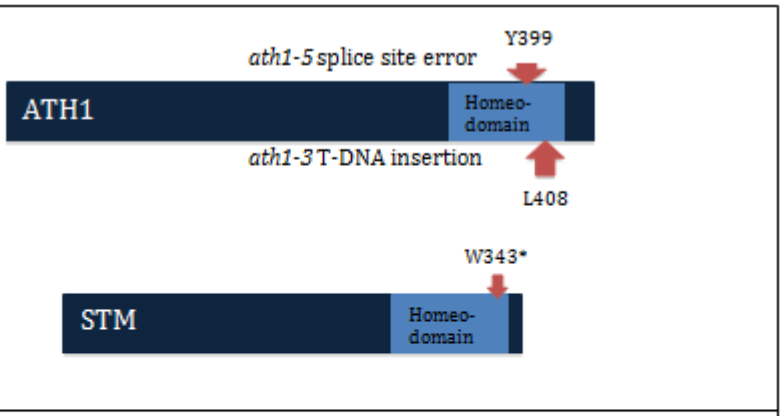

Figure 2. The *STM* and *ATH1* Transcription factor mutations occur in their homeodomain regions. The *ath1-5* allele is predicted to introduce a stop codon at position 399, while the *ath1-3* allele used in this study has a T-DNA insertion that interrupts the protein at position 409 (Gomez-Mena and Sablowski, 2008). The reduced function *stm* allele used in this study introduces a stop codon at position 343 (Liljegren, unpublished results).

Although it functions in the nucleus to control transcription of DNA, STM lacks a nuclear localization signal (Cole et al., 2006). Since STM is not able to move from the cytoplasm of a cell to the nucleus on its own, it must heterodimerize with BELL-type homeodomain transcription factors that have a nuclear localization signal in their amino acid sequence (Cole et al., 2006; Rutjens et al., 2009). ATH1 is known to be one of the BELL-type partners of STM and is found in both the cytoplasm and the nucleus of the cell (Rutjens et al., 2009). Loss-of-function *ath1*mutants do not show significant changes in the phenotype of the shoot meristem unless combined with partial loss-of-function mutations in *STM*. When the two mutations are combined,

the SAM is found to be significantly smaller (Rutjens et al., 2009). This result suggests the possibility of redundant gene function between *STM* and *ATH1*. Two other BELL-type proteins, POUND-FOOLISH (PNF) and PENNYWISE (PNY) have been shown to physically interact with STM, and genetic evidence suggests that they also share redundant activity with ATH1 in shoot meristem function. A triple *ath1 pnf pny* mutant, like the loss-of-function *stm* mutant, is missing a SAM (Rutjens et al., 2009).

Previous studies (Raybourn, 2016; Palmer, 2018) have revealed that STM and ATH1 exhibit redundancy in establishing the lateral organ boundaries of *Arabidopsis* flowers (Raybourn, 2016). When plants contain both the hypomorphic *stm* allele and the *ath1-5* allele, the boundaries that divide the sepals from the floral stem are essentially erased (**Figure 3**). Recent research in the lab has shown that the *stm ath1-5* double mutants also have significant defects in forming inter-organ boundaries, particularly between adjacent sepals and stamens (Malone, 2018).

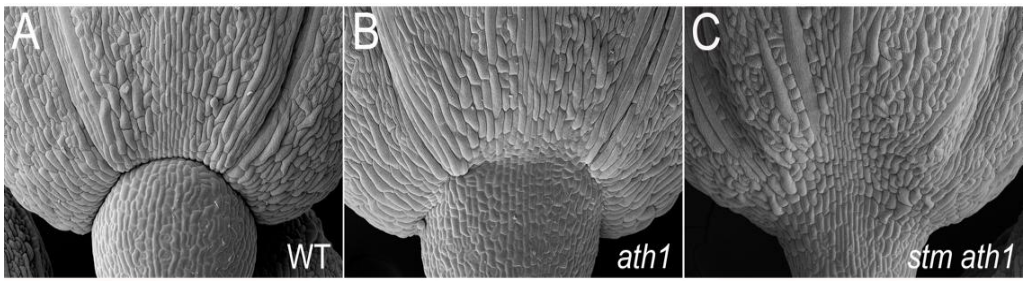

Figure 3: The sepal-stem boundary is abolished in *stm ath1* flowers. Scanning electron micrographs of a wild-type and mutant flowers. (**A**) A well-defined boundary is formed between the sepals and stem of wild-type flowers. (**B**) In *ath1* single mutant flowers, this organ boundary is less distinct. (**C**) In *stmath1-5* double mutant flowers, this boundary is absent. (Liljegren, unpublished results)

The goal of my project was to investigate the roles that the ATH1 and STM transcription factors play in establishing the inter-organ boundaries that are formed between adjacent organs of *Arabidopsis* flowers. My experiments were primarily designed to test whether an independent loss-of-function allele, *ath1-3,* behaves like the *ath1-5* allele in disrupting the boundaries formed between adjacent stamens and sepals when combined with the partial loss of function *stm* allele studied in the lab. My hypotheses were that 1) the *ath1-3* single mutants would contain a significantly higher amount of stamen-stamen fusion events when compared to wildtype plants, 2) the *stm ath1-3* double mutants would show a significantly higher amount of sepal-sepal fusion events than the single mutants and wildtype flowers. In order to test these hypotheses, I evaluated the number of organ fusion events that occurred in *stm*, *ath1-3,* and *stm ath1-3* mutant flowers compared to wildtype flowers.

It is known through previous studies that ATH1 and STM share some redundancy in maintaining a specific number of stem cells in the SAM and floral meristem of the plants

(Jasinski et al., 2005; Yanai et al., 2005). It is these stem cells that eventually develop into floral organs in *Arabidopsis thaliana.* As *STM* has an important role in maintaining these stem cell counts, I expected that plants containing the *stm* allele with reduced function will produce fewer floral organs than the wildtype plants. I also expected the *stm ath1-3* double mutants will show fewer organs than both the single *stm* mutant and the wildtype plants. To test these expectations, I counted the number of floral organs produced by these mutants compared to wildtype. By assessing both the number of fusion events found in flowers as well as the number of floral organs, the ratio of floral organs affected by fusion events could be determined.

METHODS

I. Initial Preparation of *Arabidopsis thaliana* seeds

As an experiment revolving around analyzing different genotypic traits of *Arabidopsis thaliana*, the first step was to properly plant out seeds. In order for this species' seeds to germinate properly, they needed to undergo a sterilization procedure and cold treatment prior to being planted. The sterilization procedure was initiated by covering the seeds with 70% ethanol solution for two minutes. After removing the ethanol, the seeds were covered with 5% bleach and 1% Sodium Dodecyl Sulfate solution for 15 minutes. Following this, the seeds were washed twice using approximately 500 μL of distilled and deionized water, refrigerated at 4 °C for 48 hours, then suspended in a 0.1% agarose solution and planted. For this research project, four types of seeds expected to generate four different genotypes were planted into trays and grown with a repeating cycle of sixteen hours of light followed by eight hours of darkness. The plants were kept at a temperature of approximately 23 °C and 69-70% humidity. The seeds were grown in Promix BX soil and were watered every Monday, Wednesday and Friday alternating between water and water with 200 ppm Miracle Grow. Landsberg *erecta* (Ler) plants grown in one tray were used as a wildtype (wt) control for the experiment. Two other trays contained homozygous *stm* and homozygous *ath1-3* mutant plants, respectively. Additional trays were planted to generate homozygous *stm ath1-3* double mutant plants. The double mutants studied have been found to be infertile (Liljegren, unpublished results) so seed stocks that were homozygous for one mutant and heterozygous for the other mutant were used. Knowing that these genes are not linked, according to Mendelian genetics, approximately 25% of the plants grown from this seed stock were expected to be homozygous for both of the mutant alleles. Since the germination rate of this stock had not been recently tested, we planted four trays of plants of either *stm/+ ath1-3*

or *stm ath1-3/+* heterozygous plants to assure a large enough sample size of double mutant plants. The specific seed stocks used are shown in **Table 1**.

Table 1: Seed Stocks Used for Experimentation

Seed Stock Name	# of Trays Planted	Date Collected	Possible Genotypes
"Ler WT"	1	5/25/2017	WT
"ath1-3 #1"	2	3/31/2017	*ath1-3*
"sta1 A"	2	11/27/2017	*stm*
"ath1-3 x sta1/+ #9 F4"	1	10/19/2016	*stm ath1-3, stm/+ ath1-3, STM ath1-3*
"ath1-3 x sta1/+ #15 F4"	1	10/11/2016	*stm ath1-3, stm/+ ath1-3, STM ath1-3*
"ath1-3/+ x sta1 F5"	2	1/5/2017	*stm ath1-3, stm ath1-3/+, stm ATH1*

II. Determination of Genotypes for Individual Plants

After the plants had grown for four weeks, genomic DNA was prepared so that it could be analyzed and the genotypes verified. Genomic DNA was isolated using the protocol for the QIAGEN DNeasy Plant Mini Kit with the following procedure. Collected leaf tissue from plants that were later used for phenotypic analyses was disrupted using a motorized pestle pulverizer and 400μL of AP1 buffer to break down the lipid membrane and lyse the cells. Following this, four μL of RNase was added to degrade any RNA that could be found in the mixture. This mixture was vortexed and incubated for ten minutes at 65 °C to continue breaking down the cells. After the incubation was complete, 130 μL of Buffer P3 was combined with the mixture to precipitate polysaccharides and proteins before the mixture was vortexed once again and incubated in ice for five minutes. After the cold incubation was complete, the mixtures were placed in a centrifuge and spun for seven minutes at 14,000 rpm so that the tissue debris could fully separate from the liquid and pellet at the bottom of the tube. Using a pipette, the supernatant containing the DNA was transferred into a clean QIAshredder spin column. The spin

column was then centrifuged for two minutes at 14,000 rpm to further filter out the remaining proteins and cell remnants. Next the filtrate was combined with approximately 660μL of buffer AW1, which ensured denaturation of the proteins in the mixture, and mixed by pipetting. 650μL of this mixture was placed into a DNeasy spin column and centrifuged twice at 8,000 rpm for one minute each time. Following this, 500 μL of a salt removing buffer (AW2) was added, and the mixture was once again placed in the centrifuge and spun at 8,000 rpm for one minute; this process was repeated a second time. In the final step, 100 μL of buffer AE was used to elute the DNA from the spin column followed by a five minute incubation period at room temperature. This step was repeated once to maximize the yield of DNA. The prepared samples of genomic DNA were stored at -20 °C.

Once the DNA was isolated from the plants, specific regions of the *STM* and *ATH1* genes were amplified using Polymerase Chain Reaction (PCR). The forward and reverse primers used for genotyping the *stm* and *ath1-3* mutants are shown in **Table 2**. Since the *ath1-3* mutation contains a large T-DNA insertion two separate PCR reactions were run, one designed to show the presence of the wildtype allele and the other to show the presence of the mutant allele. The PCR reactions included 18 μL of a master mix containing two μL 10X reaction buffer, 0.5 μL of 10 mM dNTP, 0.5 μL of 10X Taq polymerase, 0.7 μL each of 20 mM forward and reverse primers and 13.6 μL of distilled, deionized H_2O. Two μL of each DNA sample was then added to separate PCR tubes to bring the reaction volume to 20 μL. The samples were then loaded into and run on a S1000 ThermoCycler using program cycles optimized for each primer pair (**Table 3**).

Table 2: Primer Sequences

Primer	**5' to 3' Sequence**
ath1-3A -Used with the ath1-3B primer to amplify the wild-type ATH1 allele	CCATCAGATTTGGAGACCTAACG
ath1-3B -Used with the JMLB1 primer to amplify the mutant allele	GAGACACACTCTATATCATTTGCC
JMLB1 -anneals to one of the T-DNA borders.	CAGCTGTTGCCCGTCTCACTGGTG
STAMgtF	GTTCATAAACCAGAGGAAACGGCACTG
STAMgtR	GAGGAGATGTGATCCATTGGGAAAGG

Table 3: PCR Conditions for *STM* and *ATH1* Gene Amplification

	STM		*ATH1* WT		*ath1-3 Mutant*	
Step	**Temp. (°F)**	**Time (minutes)**	**Temp. (°F)**	**Time (minutes)**	**Temp. (°F)**	**Time (minutes)**
1	94.0	4:00	94.0	4:00	94.0	4:00
2	94.0	0:30	94.0	0:30	94.0	0:30
3	54.0	0:30	53.0	0:30	53.0	0:30
4	72.0	0:30	72.0	0:40	72.0	0:30
5	Repeat Step 2 x30	Repeat Step 2 x30	Repeat Step 2 x30	Repeat Step 2 x30	Repeat Step 2 x30	Repeat Step 2 x30
6	4.0	Indefinite	4.0	Indefinite	4.0	Indefinite

Restriction enzyme digests of the STM PCR products were then used to distinguish the mutant genotypes from wild-type. The digests included 17 µL of the PCR product, one µL of BsrI restriction enzyme and two µL of the10X 3.1 restriction enzyme buffer. This restriction

enzyme recognized and cut the wild-type PCR product into 106 bp and 29 bp fragments. The digests were incubated for four hours at 67 °C.

The sizes of the digested STM PCR products were analyzed using gel electrophoresis. Three percent agarose gels were made using six grams of agarose powder combined with 200 milliliters of 1X TAE buffer and 5.5 μL of ethidium bromide. This mixture was melted in a microwave to dissolve the agarose, cooled, and then poured into a mold with a comb to solidify over time. The ATH1 PCR products were also run on 3% agarose gels. 3.3 μL of loading dye was mixed with each of the samples, then 13.5 μL of each DNA/dye mixture was loaded into individual wells in the agarose gel. Gels were imaged using an AlphaImager HP. Controls of known wild-type and mutant DNA were included in the PCR reactions and digests to verify the sizes of the expected wild-type and mutant DNA fragments. A 50 bp ladder was used during electrophoresis in order to determine the approximate sizes of the DNA products in the experimental samples.

III. Experimental Design

When designing this experiment, various factors were accounted for to ensure as few confounding variables as possible. All of the seed stocks were planted on the same day, and to control for any differences in seed germination and developmental progress, data were collected from stage 13-15 flowers found within the 7^{th} and 18^{th} positions on the primary inflorescence of each plant. These developmental stages encompass the time from when the buds begin to open until the pollinated fruit begins to elongate (Smyth et al., 1990). Positions were numbered with the oldest seedpod at the base of the inflorescence deemed number one, then moving up the stem in chronological order. Within the range of positions 7-18, the first flower without withering

organs (stage 15) was selected to be the first floral bud that data was collected for each plant. Each successive flower bud was then analyzed through flowers undergoing anthesis (stage 13; bud opening). Each floral bud was looked at through a dissecting microscope to determine the number of sepals, petals and stamens present as well as the number of fusion events observed between the floral organs. Every fusion event seen between two organs was recorded, regardless of whether it was partial or complete. Fusion percentage was calculated by dividing the number of floral organs affected by a fusion event by the number of organs within that flower.

IV. Data Analysis

Microsoft Excel was used to analyze the collected data. Bar graphs were generated to illustrate the average percentage of fusion for 1) sepals, 2) petals, 3) stamens and 4) all outer organs for each genotype. The number of outer floral organs per flower was also determined for each genotype tested and independently depicted via bar graph. Standard deviations of the samples and standard errors from the mean are shown in tables associated with each bar graph. Phenotypic differences between genotypes were considered statistically significant ($P < 0.05$) if the standard errors of their respective means did not overlap.

RESULTS

Each individual flower was analyzed using a dissecting microscope to record the number of floral organs produced and to identify any inter-organ fusion events. I was able to examine 40 flowers each for the *stm* mutant, the *ath1-3* mutant and wild-type plants; 25 flowers were examined for the *stm ath1-3* double mutants. Fewer healthy plants with flowers at the right stage were available from the set of double mutants grown for this experiment. Data were collected from ten plants each for the wildtype and single mutant plants but only from four double mutant plants. On average, four flowers were assessed per plant for the wildtype, *stm* mutant, and *ath1-3* mutant while six flowers per plant were evaluated for the double mutant plants.

After collecting the data, I determined the frequency of inter-organ fusion events and compared the number of floral organs produced by the flowers of each genotype. In order to calculate fusion percentage, the number of organs with fusion defects was divided by the total number of that organ type. For instance, if there were two pairs of fused stamens within a flower, 100% of its stamens were recorded as fused.

The frequency of stamen-stamen fusion was higher in the single mutants compared to wild-type flowers, with 15% of *ath1-3* and *stm* stamens showing a fusion defect compared to 0% of wild-type stamens. This phenotype was enhanced in the double mutant, with 51% of the *stm ath1-3* stamens fused to another stamen (**Figure 4**).

Frequency of Stamen Fusion			
	Mean	**St dev.**	**St. Error**
WT	0	0	0
Stm	14.75	21.05	3.33
ath1-3	14.75	21.39	3.38
stm ath1-3	51.47	46.33	9.27

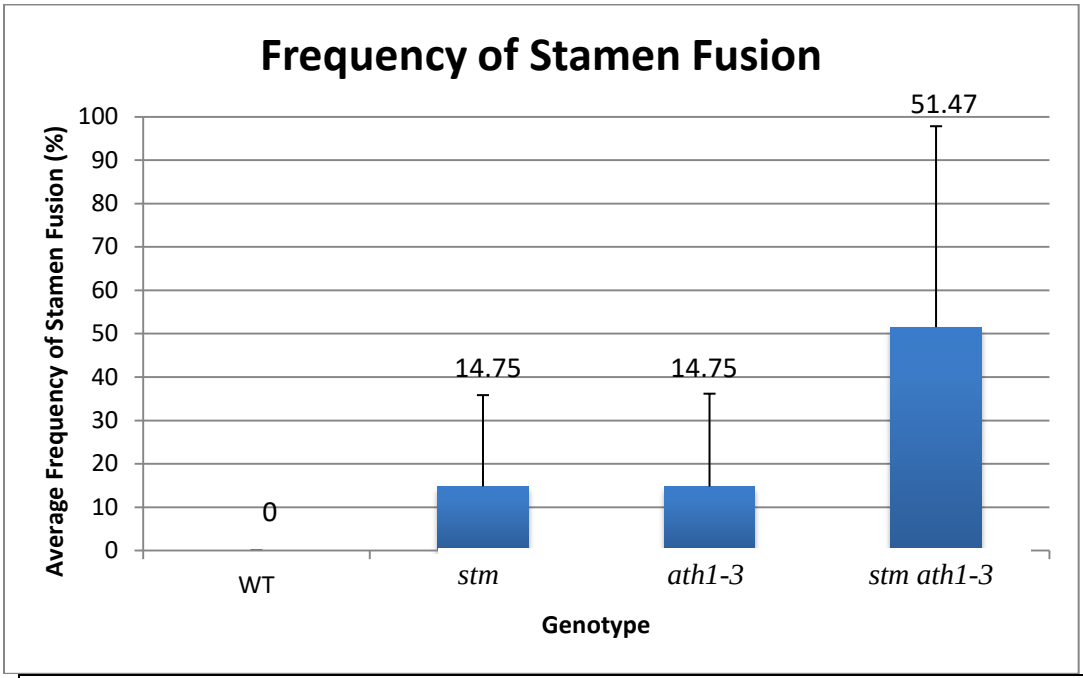

Figure 4: Frequency of Stamen Fusion. n=40 for WT. n=40 for *stm* single mutant flowers. n=40 for *ath1-3* mutant flowers. n=25 for *stm ath1-3* double mutant flowers. This graph shows the average frequency of stamen-stamen fusion events in each sample group. Error bars indicate standard deviation. The average fusion frequency for each group is portrayed above the respective bars on the graph. The single and double mutant flowers show significantly more fusion events than the WT plants.

The frequency of sepal-sepal fusion showed a stark contrast when comparing the double mutant plants to the wildtype and single mutant plants. The sepals in the double mutant flowers were almost universally fused (95%), while the sepals of the *stm* mutant and wildtype flowers were never fused (0%), and the sepals of the *ath1-3* flowers were rarely fused (1%) **(Figure 5)**.

Frequency of Sepal Fusion			
	Mean	**St. Dev.**	**St. Error**
WT	0	0	0
stm	0	0	0
ath1-3	0.625	3.95	0.625
stm ath1-3	94.67	13.15	2.63

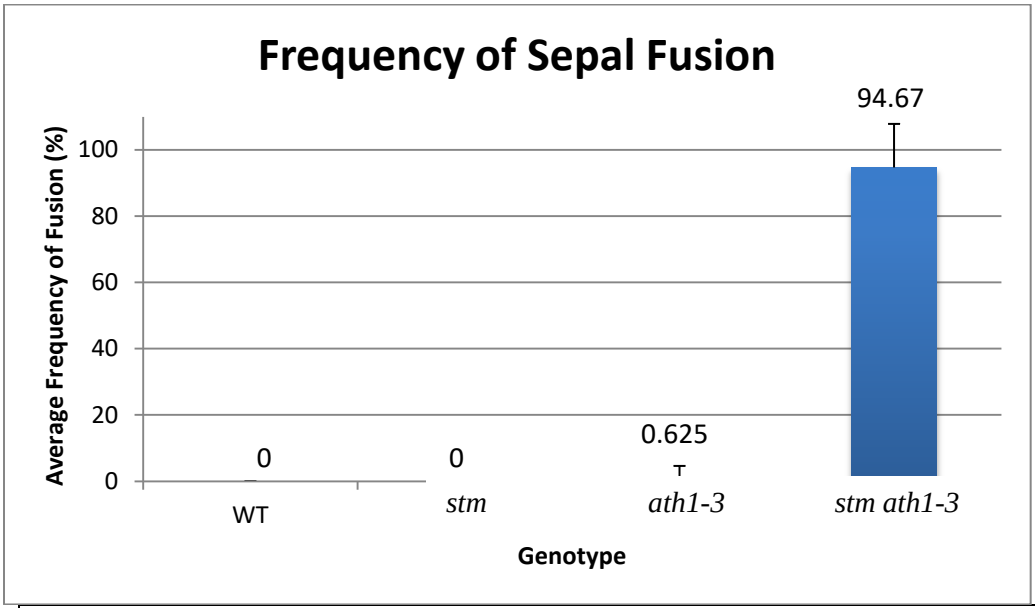

Figure 5: **Frequency of Sepal Fusion.** n=40 for WT. n=40 for *stm* single mutant flowers. n=40 for *ath1-3* mutant flowers. n=25 for *stm ath1-3* double mutant flowers. This table and bar graph shows the average frequency of sepal-sepal fusion events in each sample group. Error bars indicate standard deviation. The average fusion frequency for each group is portrayed above the respective bars on the graph. The double mutant flowers demonstrate significantly more fusion events than the WT and single mutant plants.

Considering all of the outer organs (**Figure 6**), 58% of the organs in the *stm ath1-3* double mutants were affected by fusion events, compared to 3% of the organs in both single mutants, and 0% of the organs in the wild-type flowers .Fusion events affecting organs in adjacent whorls (i.e. petal-petal, sepal-petal, and petal-stamen) were searched for but not observed in the mutants analyzed during this experiment.

Frequency of Total Fusion			
	Mean	**St. Dev.**	**St. Error**
WT	0	0	0
stm	2.99	4.37	0.69
ath1-3	3.08	4.16	0.66
stm ath1-3	57.92	18.48	3.70

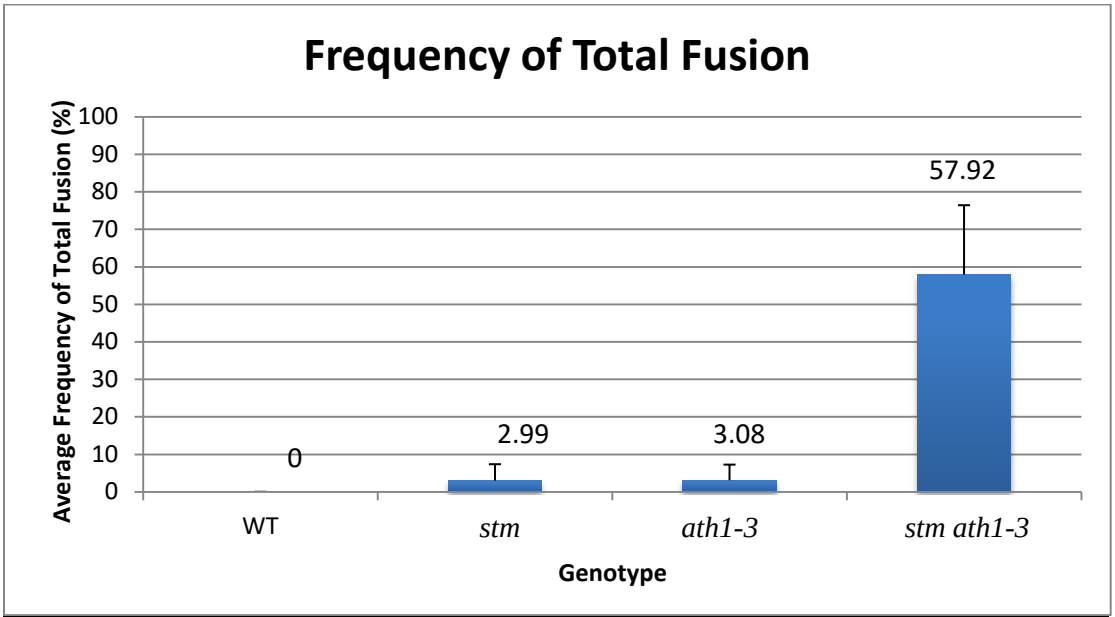

Figure 6: Frequency of Total Fusion. n=40 for WT. n=40 for *stm* single mutant flowers. n=40 for *ath1-3* mutant flowers. n=25 for *stm ath1-3* double mutant flowers This table and bar graph shows the average frequency of total fusion events in each sample group. Error bars indicate standard deviation. The average fusion frequency for each group is portrayed above the respective bars on the graph. The double mutant flowers demonstrate more significantly more fusion events than the WT and single mutant plants.

To determine if there was variation between the different genotypes, the number of floral organs in each flower was also recorded. No significant differences were detected between the number of sepals produced (**Figure 7**); flowers from the wildtype plants, *stm* and *ath1* single mutants and *stm ath1* double mutant each produced an average of 4 sepals.

Average # of Sepals			
	Mean	**St. Dev.**	**St. Error**
WT	3.975	0.16	0.025
stm	4	0	0
ath1-3	4	0	0
stm ath1-3	3.88	0.44	0.09

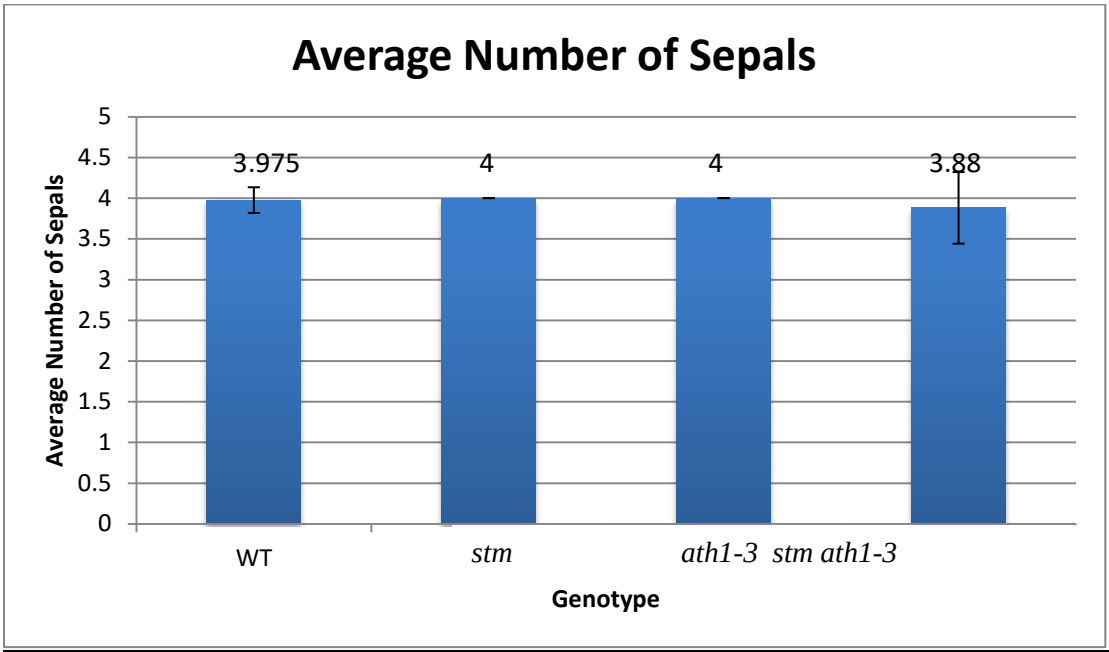

Figure 7: Average Number of Sepals. n=40 for WT. n=40 for *stm* single mutant flowers. n=40 for *ath1-3* mutant flowers. n=25 for *stm ath1-3* double mutant flowers. This bar graph shows the average number of sepals on flowers of each sample group. The error bars indicate standard deviation. The average number of sepals found in each genotype is portrayed above the respective bars on the graph. The difference between the numbers of sepals produced is not significant.

The single mutant plants did not demonstrate significant differences in petal number when compared to the wildtype plants (**Figure 8**); flowers of each genotype contained an average of 4 petals. However, the double mutant plants produced significantly fewer petals than either the wild-type or the single mutants, with an average of 1 petal per flower **(Figure 8)**.

Average # of Petals			
	Mean	**St. Dev.**	**St. Error**
WT	4	0	0
stm	3.95	0.22	0.035
ath1-3	3.98	0.16	0.025
stm ath1-3	1.32	1.31	0.26

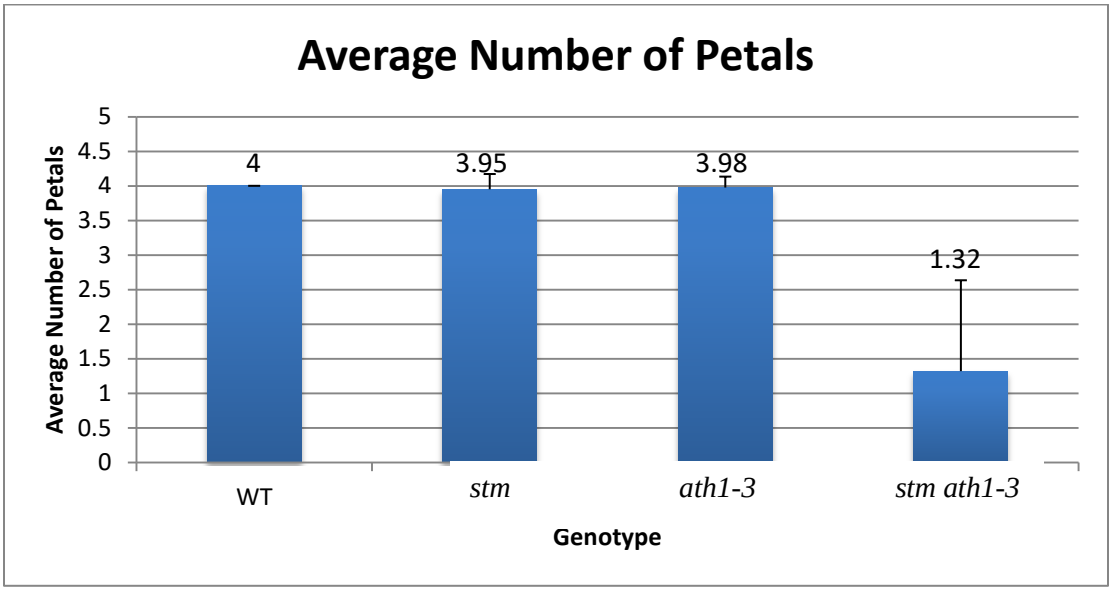

Figure 8: Average Number of Petals. n=40 for WT. n=40 for *stm* single mutant flowers. n=40 for *ath1-3* mutant flowers. n=25 for *stm ath1-3* double mutant flowers. This bar graph shows the average number of petals on flowers of each sample group. The error bars indicate standard deviation. The average number of petals found per sample group is portrayed above the respective bars on the graph. The *stm ath1-3* double mutant flowers produced significantly less petals per flower than either single mutant or wildtype.

The single mutant plants produced on average one fewer stamen compared to the wild-type plants (**Figure 9**).Compared to the wild-type average of 6 stamens, the *stm* and *ath1* flowers produced an average of 5 stamens. The double mutant flowers produced significantly fewer stamens than either the single mutants or wild-type, with an average of 3 stamens (**Figure 9).**

Average # of Stamen			
	Mean	**St. Dev.**	**St. Error**
WT	5.85	0.36	0.06
stm	4.98	0.73	0.12
ath1-3	5.25	0.63	0.10
stm ath1-3	3.20	1.58	0.32

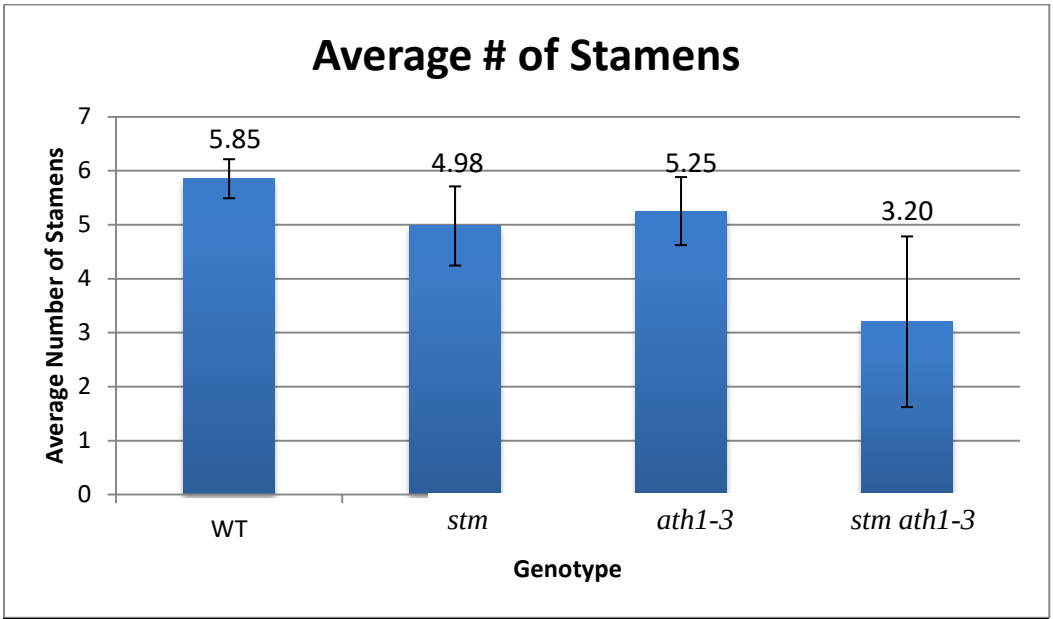

Figure 9: Average Number of Stamen. n=40 for WT. n=40 for *stm* single mutant flowers. n=40 for *ath1-3* mutant flowers. n=25 for *stm ath1-3* double mutant flowers. This bar graph shows the average number of stamens on flowers of each sample group. The error bars indicate standard deviation. The average number of stamens found per sample group is portrayed above the respective bars on the graph. The *stm ath1-3* double mutant flowers produced significantly fewer stamens on average compared to wildtype.

The total number of outer floral organs produced per flower (sepals, petals, and stamens) was calculated for each genotype (**Figure 10**). Both of the single mutants contained one fewer organ per flower on average than wild-type, with 13 total organs compared to 14, respectively. The *stm ath1-3* double mutant flowers produced significantly fewer organs than either the single mutants or wild-type, with an average of 8 total organs (**Figure 10)**.

Average of Total Floral Organs				
	Total # of Floral Organs	**Mean Per Flower**	**St. Dev**	**St. Error**
WT	553	13.83	0.91	0.14
stm	517	12.93	0.65	0.10
ath1-3	529	13.23	0.70	0.11
stm ath1-3	210	8.40	1.62	0.26

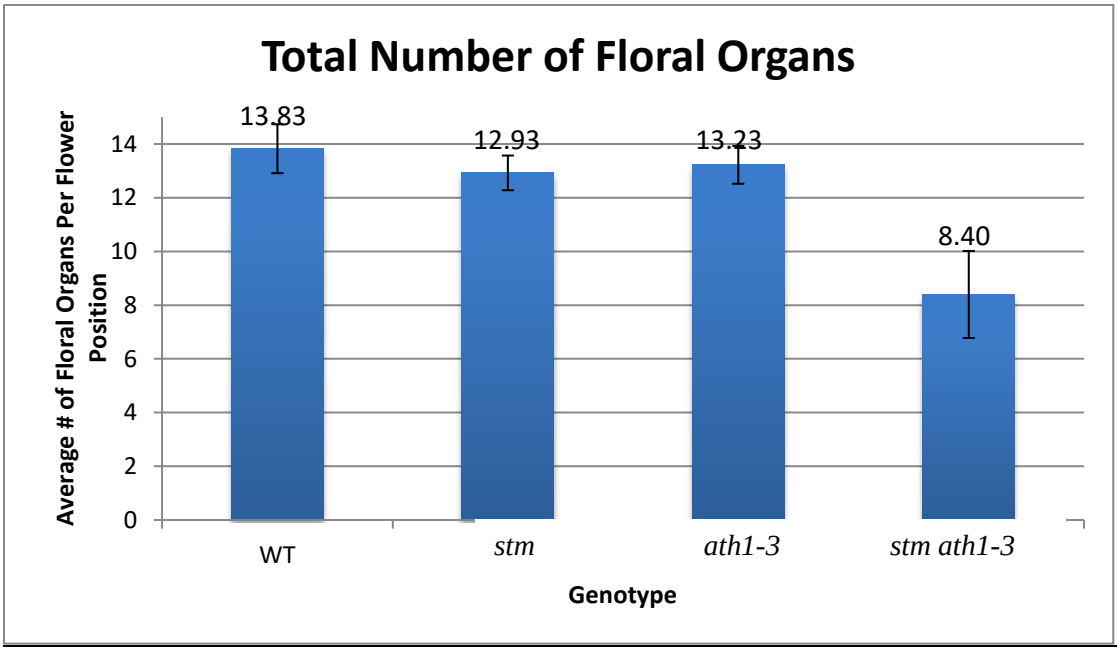

Figure 10: Total Number of Floral Organs. n=40 for WT. n=40 for *stm* single mutant flowers. n=40 for *ath1-3* mutant flowers. n=25 for *stm ath1-3* double mutant flowers. This bar graph shows the average total number of floral organs found on flowers of each sample group. The error bars indicate standard deviation. The average number of total organs found per sample group is portrayed above the respective bars on the graph. The *stm ath1-3* double mutants produce significantly fewer floral organs than either single mutant or wildtype.

DISCUSSION

Prior research regarding the roles that the STM and ATH1 transcription factors play in both development of inter-organ boundaries and the formation of floral organs was the motivating factor in selecting the topic of my research experiment. The hypothesis that STM and ATH1have significant roles in forming the boundaries between individual floral organs as well as the boundaries between the floral organs and underlying receptacle was initially tested using the *ath1-5* allele (Malone, 2018). I hypothesized that if ATH1 truly plays a critical role in establishing the inter-organ boundaries formed between the sepals and stamens, I would observe 1) a significantly increased number of stamen-stamen fusion events in the single *ath1-3* and double *stm ath1-3* mutants compared to wild-type and 2) a significantly increased number of sepal-sepal fusion events in the *stm ath1-3* double mutant compared to the single mutants and wild-type.

The data I collected supported my first hypothesis that disruption of ATH1 activity using an independent allele from one previously tested would disturb the boundaries formed between adjacent stamens. My results were particularly striking for the *stm ath1-3* double mutant, in which 51% of the stamens were fused to another stamen compared to 0% of wild-type stamens (see **Figure 4)**. As 15% of the stamens in the *ath1-3* single mutant were also affected by fusion events, significantly higher frequencies of stamen-stamen fusion events were observed for both the single and the double mutant compared to wild-type.

My second hypothesis that ATH1 and STM are redundantly responsible for maintaining the boundaries between adjacent sepals was strongly supported by my data (see **Figure 5**). Whereas 95% of the sepals in the double mutant were fused, only 1% of the sepals in the *ath1* single mutant, and none of the sepals in the *stm* single or wild-type plants showed fusion defects.

These results suggest that ATH1 and STM are able to function independently in establishing the inter-organ boundaries formed between sepals. When the function of the ATH1 transcription factor alone is disrupted, these boundaries was not significantly altered compared to those of wild-type plants. However, when the function of the STM transcription factor is also disrupted in the double mutant flowers, the sepal-sepal boundaries are significantly disturbed compared to either the single mutants or to the wildtype.

Although I also looked for any fusion events affecting floral organs in adjacent whorls, all the fusion defects I found occurred between neighboring floral organs within the same whorl. The boundary regions that separated different whorls were not found to be significantly affected in *stm ath1-5* plants either (Malone, 2018), thus it appears unlikely that these transcription factors are involved in establishing inter-whorl boundaries. Instead, it appears that STM and ATH1primarily regulate the inter-organ boundaries formed in the outermost whorl of sepals and the inner whorl of stamens. No fusion events were detected in the petals of the *ath1-3* or *stm ath1-3* flowers.

The results from this study also support my hypotheses that STM and ATH1 play important roles in regulating the maintenance of the flower meristem. While the number of sepals did not show any significant differences between the mutants I studied, the number of petals and stamens were significantly reduced by the combined presence of the *stm* and *ath1-3* mutations. On average, the *stm ath1-3* double mutant flowers contained about five fewer organs than the wildtype flowers, and were missing at least two petals and two stamens. This was expected as STM has a known function in maintaining stem cell numbers in the SAM as well as in floral meristems (Jasinski et al., 2005; Yanai et al., 2005). After comparing this previously known information with the recently collected data it appears that the STM and

ATH1transcription factors share roles in maintaining the number of stem cells that must be present within the floral meristem in order to generate the four sepals, four petals, six stamens and a central pistil typically found in an *Arabidopsis* flower.

When designing this study, it was not known in advance whether the *ath1-3*and *ath1-5* alleles would show any differences in their phenotypes. Since Gomez-Mena and Sablowski (2008) had concluded that the *ath1-3* allele was a loss-of-function allele, and it wasn't clear whether the *ath1-5* allele should be considered as a loss-of-function or hypomorphic allele, an initial hypothesis was that the phenotypic effect of the *ath1-3* mutation would be greater than that of the *ath1-5* mutation previously studied(Malone, 2018). However, after comparing the data for my project and the parallel project using the *ath1-5* allele, I didn't find any notable differences. Although the frequencies of stamen fusion in my project were approximately double that of the previous study, it is noteworthy that the percentage of fusion events per floral organ were calculated in a different way (Malone, 2018). For instance if two stamens were fused, they were counted as one fusion event/two organs, or 50%, whereas I would count that as 100% fusion. Furthermore, when comparing the organ counts, no significant difference were found between any of the plants containing the *ath1-5* mutation and the plants containing the *ath1-3* mutation. My results suggest that the two alleles may be functionally equivalent.

There are multiple directions that this research can take in the future. For instance, the extent to which the edges of the sepals and stamens are fused in the *stm ath1* double mutant could be determined. An interesting feature I noticed about the *stm ath1* double mutants is that the distance between the positions of individual flowers along the primary stem appeared to be closer to one another than those that grow on primary stems of wildtype and single mutant plants. This observation could be tested and quantified in order to determine if there is a

significant reduction in internode length when STM and ATH1 function is compromised. The results of my analysis of the number of floral organs produced by *ath1-3* and *stm ath1-3* mutant flowers compared to wild-type flowers will help refine the analysis of abscission defects in these mutants. My results also have relevance to a study investigating whether the *ath1-3* and *stm ath1-3* mutants have a higher retention of floral organs due to their lateral organ boundary defects (Roth, 2018). Since the number of organs a flower produces affects the number it is capable of retaining, my analysis will help put the results from this study and future studies in context.

WORKS CITED

Aida, M., Ishida, T. and Tasaka, M. (1999). Shoot apical meristem and cotyledon formation during *Arabidopsis* embryogenesis: Interaction among the *CUP-SHAPED COTYLEDON* and *SHOOT MERISTEMLESS* genes. *Development* 126, 1563–1570.

Arnaud, N. and Pautot, V. (2014). Ring the BELL and tie the KNOX: roles for TALEs in gynoecium development. *Front. Plant Sci.* 5, 93.

Barton, M. K. (2010). Twenty years on: The inner workings of the shoot apical meristem, a developmental dynamo. *Developmental Biology* 341, 95-113.

Breuil-Broyer, S., Morel, P., de Almeida-Engler, J., Coustham, V., Negruitiu, I. and Trehin, C. (2004). High-resolution boundary analysis during *Arabidopsis thaliana* flower development. *Plant Journal* 38, 182–192.

Cole, M., Nolte, C. and Werr, W. (2006). Nuclear import of the transcription factor SHOOT MERISTEMLESS depends on heterodimerization with BLH proteins expressed in discrete sub-domains of the shoot apical meristem of *Arabidopsis thaliana*. *Nucleic Acids Research* 34, 1281–1292.

Endrizzi, K., Moussian, B., Haecker, A., Levin, J. Z. and Laux, T. (1996). The *SHOOT MERISTEMLESS* gene is required for maintenance of undifferentiated cells in *Arabidopsis* shoot and floral meristems and acts at a different regulatory level than the meristem genes *WUSCHEL* and *ZWILLE*. *Plant Journal*10, 967–979.

Gomez-Mena, C., and Sablowski. R. (2008). *ARABIDOPSIS THALIANA HOMEOBOX GENE1* establishes the basal boundaries of shoot organs and controls stem growth. *The Plant Cell* 20, 2059–2072.

Gubert, C. M., Christy, M. E., Ward, D. L., Groner, W. D. and Liljegren, S. J. (2014). ASYMMETRIC LEAVES1 regulates abscission zone placement in *Arabidopsis* flowers. *BMC Plant Biology* 14, 195.

Irish, V. F. (1999). Patterning the flower. *Developmental Biology*209, 211–220.

Jasinski, S., Piazza, P., Craft, J., Hay, A., Woolley, L., Rieu, I., Phillips, A., Hedden, P. and Tsiantis, M. (2005). KNOX action in *Arabidopsis* is mediated by coordinate regulation of cytokinin and gibberellin activities. *Current Biology* 15, 1560-1565.

Long, J. A., Moan, E. I., Medford J. I., and Barton, M. K. (1996). A member of the KNOTTED class of homeodomain proteins encoded by the *STM* gene of *Arabidopsis*. *Nature* 379, 66-69.

Malone, H. (2018). Characterizing the effects of mutations in *STM* and *ATH1*on floral organ development in *Arabidopsis thaliana*. Undergraduate honors thesis, Department of Biology, University of Mississippi.

Meinke, D. W., Cherry, J. M., Dean, C., Rounsley, S. D. and Koornneef, M. (1998). *Arabidopsis thaliana*: a model plant for genome analysis." *Science* 282, 679-82.

Palmer, S. (2018). Quantifying abscission defects in mutant *Arabidopsis thaliana* flowers. Undergraduate honors thesis, Department of Biology, University of Mississippi.

Raybourn, D. (2016). Investigation of the expression of the *HAESA* receptor-like kinase as regulated by the STM and ATH1 homeodomain transcription factors in *Arabidopsis thaliana.* Undergraduate honors thesis, Department of Biology, University of Mississippi.

Roth, H. (2018). The effect of mutations in the *ATH1* and *STM* genes on sepal, petal, and stamen abscission in *Arabidopsis thaliana* plants. Undergraduate honors thesis, Department of Biology, University of Mississippi.

Rutjens, B., Bao, D., van Eck-Stouten, E., Brand, M., Smeekens, S. and Proveniers, M. (2009). Shoot apical meristem function in Arabidopsis requires the combined activities of three BEL1-like homeodomain Proteins. *Plant Journal* 58, 641–654.

Scofield, S., Dewitte, W. and Murray, J. A. (2014). STM sustains stem cell function in the *Arabidopsis* shoot apical meristem and controls *KNOX* gene expression independently of the transcriptional repressor AS1. *Plant Signaling & Behavior* 9, e28934.

Shuai, B., Reynaga-Pena, C. G. and Springer, P. S. (2002). The *Lateral Organ Boundaries* gene defines a novel, plant-specific gene family. *Plant Physiology* 129, 747-6.

Smyth, D. R., Bowman, J. L. and Meyerowitz, E. M. (1990). Early flower development in *Arabidopsis*. *Plant Cell* 2, 755-67.

Yanai, O., Shani, E., Dolezal, K., Tarkowski, P., Sablowski, R., Sandberg, G., Samach, A. and Ori, N. (2005). *Arabidopsis* KNOXI proteins activate cytokinin biosynthesis. *Current Biology* 15, 1566–1571.